Proceedings of the 2006 IEEE/RSJ
International Conference on Intelligent Robots and Systems
October 9 - 15, 2006, Beijing, China

Multiscale Sensing: A new paradigm for actuated sensing of high frequency dynamic phenomena

Amarjeet Singh, Diane Budzik, Willie Chen,
Maxim A. Batalin, Michael Stealey, Henrik Borgstrom and William J. Kaiser
Electrical Engineering Department
Center for Embedded Networked Sensing
University of California Los Angeles, Los Angeles, California 90095

Abstract— **Many environmental applications require high temporal frequency (rapidly changing) and spatially distributed phenomena to be sampled with high fidelity. This requires mobile sensing elements to perform guided sampling in regions of high variability. We propose a multiscale approach for efficiently sampling such phenomena. This approach introduces a hierarchy of sensors according to the sampling fidelity, spatial coverage, and mobility characteristics. In this paper, we report the development of a two-tier multiscale system where information from a low-fidelity, high spatial (global) sensor actuates a mobile robotic node, carrying a high-fidelity, low spatial coverage (spot measurement) sensor, to perform guided sampling in the regions of high phenomenon variability. As a case study of the proposed multiscale paradigm, we investigated the spatiotemporal distribution of the light intensity in a forest understory. The performance of the multiscale approach is verified in simulation and on a physical system. Results suggest that our approach is adequate for the problem of high-frequency spatiotemporal phenomena sampling and significantly outperforms traditional sampling approaches such as a raster scan.**

I. Introduction

A broad class of applications including environmental sampling, public health environment monitoring, precision agriculture, and security require distributed sensing capabilities [1]. This requirement is attributed to the high frequency spatiotemporal distribution of the sensing phenomena. Characterizing such phenomena with only static sensors requires an impractically large number of sensors to be distributed across the complete spatial extent of the sampled phenomena. For example, solar radiation and atmospheric properties that display variability on a centimeter scale are often required to be mapped over a large spatial area within a forest (typical width of 50 m and length of 100 m). High fidelity sampling of such phenomena over a two dimensional plane with a required spatial coverage of over 1000 m^2 and with a required resolution greater than 10 samples/m^2 requires a deployment of sensors that is not only excessively costly in resources, but is also potentially a source of disturbance to the environment under investigation.

Mobile sensing elements (mobile robots equipped with sensors) offer an alternative to a network of static sensing elements for high spatial coverage but at the cost of increased delay (sampling latency). One approach to reduce such latency is to apply an *adaptive sampling* technique [2], [3], which is a multi-step approach that varies sampling density at each step. In such algorithms, during the first step a mobile robot performs a coarse scan of the complete environment to extract the regions of high phenomenon variability. Then, selected regions are sampled with higher density to improve the overall sampling fidelity. Adaptive sampling techniques are known to perform well in cases where a phenomenon is not changing significantly. However, the latency involved in extracting the regions of interest (high variability regions) is large and makes these techniques unsuited for sampling dynamic phenomena. Note that many environmental phenomena are dynamic (e.g. solar light radiation, CO_2 flux, humidity etc.).

Another approach to reduce sampling latency is to use a combination of static sensing elements and mobile robots [4], [5]. In [4], [5] a set of n static sensors is deployed such that the environment is discretized into n regions (one sensor in each region). Next, these sensors monitor corresponding regions for events of interest (such as high concentration of a phenomenon). When an event is detected, the system is notified, and the mobile robot is tasked to sample only in the region of the sensor that triggered an event. A distributed task allocation is implemented to deal with task prioritization. This approach improves the sampling latency and can be applied to dynamic phenomena. Events occurring outside the range of a static sensor, however, might be missed in this approach. Thus, the performance of the system depends on the number of sensors (or the level of discretization of the environment). This forces a tradeoff between the high cost of the solution (too many sensors) and high fidelity of a phenomenon reconstruction. Note also that in this approach static sensors are not necessarily required to have high-fidelity characteristics, because they can only act as triggers and may not be used for sampling. Consequently, this motivates the need for a single low cost sensor that can provide low-fidelity, high spatial coverage (global) information. Such a sensor can determine regions of importance and task the mobile robots to sample in those regions, thus improving the sampling fidelity.

We propose a *multiscale approach* for efficiently sampling high frequency spatiotemporal phenomena with high fidelity. This approach introduces a hierarchy of sensors according to sampling fidelity, spatial coverage, and mobility characteristics. In this paper we focus on a study of a two-tier system. The first tier is represented by a static low-fidelity high spatial coverage sensor providing ”global” information about the environment. This information is then used to extract the regions of interest (regions of high phenomenon variability).

1-4244-0259-X/06/$20.00 ©2006 IEEE

The second tier is represented by mobile robots with high-fidelity low spatial coverage (spot measurement) sensors. The mobile robots are then actuated to perform guided sampling of the regions extracted by the first tier sensor.

We investigated spatiotemporal distribution of light intensity under a forest canopy as both an important application [6] and a verification of the proposed multiscale paradigm. We used an imager (a camera) as a first tier sensor. An imager provides a snapshot of the light distribution over the experimental area. This snapshot has high spatial coverage, but low fidelity caused by the varying surface reflectivity of the environment, the non-linearity of the imager and the small range of possible intensities (range of pixel values compared with range of the sensed phenomenon). Global information provided by the imager is used by our algorithm to guide a mobile robot equipped with a Photosynthetically Active Radiation (PAR) sensor to obtain low-resolution, high-fidelity information about incident light. Light is measured as PAR, which is defined as radiation in the 400-700 nm waveband [7]. Since the imager provides an instantaneous snapshot of the complete environment, this technique is neither dependent on the placement or the number of static sensors, nor constrained by the high frequency of the sensed phenomenon.

The output of an imager is processed to produce a set of tasks representing regions covered with sun-flecks (bright light patches). These tasks are then assigned to the mobile robots for servicing (sampling). Task Assignment is a well studied problem in Multi-Robot Task Allocation [8], and Operations Research [9]. Solutions to such a problem assume certain task characteristics. In our case, task characteristics are not known a priori. Therefore, we implemented a greedy heuristic-based task allocation algorithm where tasks are prioritized based on a utility (service time and sampled area).

We present an analysis of the performance of our approach using prerecorded real data in simulation and on an actual physical system. Note that the simulation and experiments with the real system were performed on a smaller scale compared to the scale of the sensing region in the real environment (order of $1000m^2$). The absolute performance will be worse with an increase in the sensing area. However, the overall trend of our results will still hold true: the multiscale paradigm significantly outperforms traditional sampling approaches such as a raster scan.

II. Enabling Robotic Platform

The requirement of sustainable and precise mobile sensing for environmental applications inspired the development of Networked Info-Mechanical Systems (NIMS) [10]. NIMS introduced infrastructure-supported mobility with mobile robots carrying sensors that can autonomously explore a three dimensional volume. Infrastructure supported mobility helps in precise location resolution, enabling actuation of the NIMS node to perform guided sampling. NIMS provides large spatial coverage with precise localization. These characteristics make NIMS an ideal robotic platform for studying high frequency, dynamic phenomena with high fidelity. A three dimensional

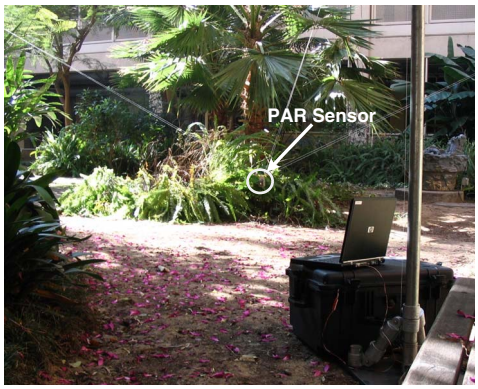

Fig. 1: NIMS-3D performing light sensing

version of NIMS, NIMS-3D [11], is shown in Figure 1. NIMS-3D is a novel, rapidly deployable cable-based robotic system capable of accurate positioning within its 3-dimensional span. The system is designed for indoor and outdoor use. The hardware is composed primarily of commercially available components. A motor powered spooling system is a major component of NIMS-3D [11]. Control of the motor system is accomplished through a PID controller that ensures precise location mapping. Motors used in the system are 24V DC sub-fractional horsepower gear motors.

When the phenomena to be characterized is changing at a rate faster than the sampling rate of the mobile robot, the constraints of the physical system, such as sampling time and average speed, limit the total amount of information that can be gathered from the environment. System performance with such constraints can be improved by sampling the environment in an intelligent way. Next, we present a multiscale approach for intelligent sampling.

III. An Overview of a Two-tier Multiscale Architecture

Multiscale sensing, proposed here, is based on a hierarchical system that enables autonomous arrangement of sensors with the objective of optimizing sensing fidelity, spatial coverage, and mobility characteristics. This system of sensors then can be used for efficient high fidelity sampling of high frequency spatiotemporal phenomena.

A two-tier multiscale system is reported here. A schematic view of its architecture is shown in Figure 2. In this architecture, high frequency dynamic phenomena is captured by a first-tier sensor. The first tier is represented by a static low-fidelity high spatial coverage sensor providing ”global” information about the environment. This information is then used to extract the regions of interest (regions of high phenomenon variability). These regions form a set of sampling tasks for the second-tier sensors to pursue. The second tier is represented by the mobile robots equipped with high-fidelity low spatial coverage (spot measurement) sensors. A set of new tasks is

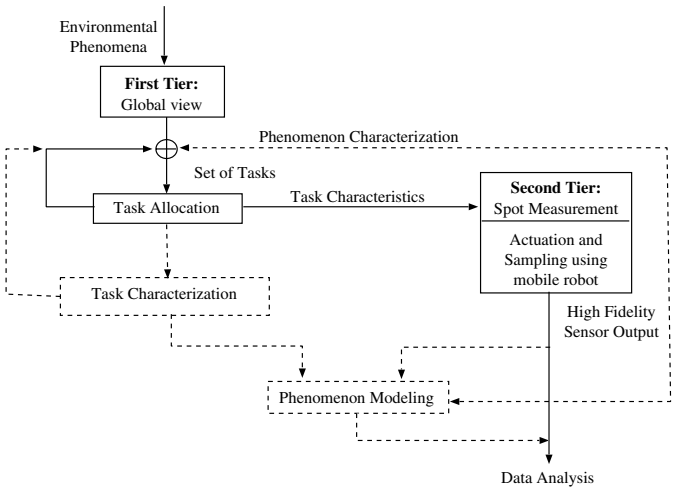

Fig. 2: An overview of a two-tier multiscale architecture. Future modules and their data flow paths are marked with dotted lines.

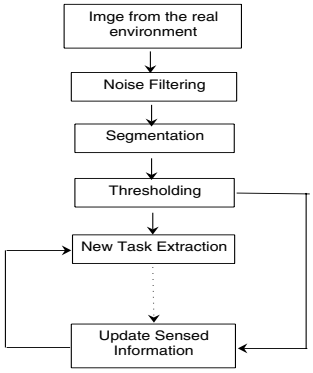

Fig. 3: Image Processing Algorithm

given as an input to the Task Allocation module. The task allocation module prioritizes tasks based on the selected utility and assigns the task with highest utility to the available mobile robot for high-fidelity sampling.

An output of the system is a set of high-fidelity phenomenon measurements in a given region, which then can be used by scientists. In the future, we plan to augment the described architecture with two new modules. The first module is Task Characterization (please refer to Figure 2). Task Charateriza-tion will collect the complete task information from the Task Allocation module and build a model of future task arrivals and distributions. Task characterization would further improve task allocation and at the limit yield an optimal solution.

Another future module is phenomenon modeling based on the received high-fidelity sensed values. This information can be used to improve first-tier sensor data processing and segmentation, as well as calibration. In theory, if the first-tier sensor is calibrated in accordance with the spatiotemporal non-linearities in the environment, the high-fidelity phenomenon information can be extracted (or much closer approximated) directly from the first-tier sensor.

IV. Sampling Light Intensity: A Case Study

Sampling light intensity under a forest canopy is used as a probe of sensing performance for multiscale actuated sensor systems. In this application, we use an imager (a camera) as a first-tier sensor. The imager is a high spatial coverage, low-fidelity sensor that provides global information about the light intensity in the environment. This information is then used to actuate the mobile robot equipped with a low spatial coverage, high-fidelity PAR (light intensity) sensor (a second-tier sensor). In this section we describe the two main modules of the system - Image Processing and Task Allocation.

A. Image Processing Module

The Image Processing Module takes as its input an image of the environment captured by the imager. Images are processed using the Open Source Computer Vision Library (OpenCV) [12]. An overview of the Image Processing algorithm is shown in Figure 3. The first step in image processing is noise filtering, which is accomplished through image down-sampling and up-sampling. Next, we perform the segmentation of an image using a pyramid segmentation algorithm [13]. The segmented color image is then converted into a gray-scale image. Then we apply a thresholding in order to achieve a bi-level (binary) image from the gray-scale image. In this binary image, white areas represent regions covered with sun-flecks (regions of importance) and black areas represent regions covered with shadow. Intermediate results of these steps are shown in Figure 4.

The final step in image processing is to extract new regions of interest. These regions form an input set of tasks to the Task Allocation module (described next). We assume that only the regions covered with sun-flecks (bright patches) are the regions of interest. Regions that were bright when sampled by the mobile robot and became covered with shadow, according to the current snapshot of the environment, were updated directly. Finally, only the regions that were previously covered with shadow and became covered with sun-flecks are extracted as tasks. This approach is motivated by a high degree of error discovered in image information for bright regions caused by non-uniform reflectivity of the captured surface. Hence, low resolution high fidelity sampling is required for bright regions.

Note that our focus in this paper is to show the importance of using a multiscale paradigm in studying high frequency spatiotemporal phenomena and not novel approaches in image processing. The performance of the image processing, however, can be further improved by applying more optimal algorithms for segmentation, thresholding, and task extraction.

B. Task Allocation

A set of tasks extracted by the Image Processing module is supplied as input to the Task Allocation module. The Multi-Robot Task Allocation (MRTA) problem has been well-studied in the robotics community [8] and, simply stated, is the problem of allocating tasks to robots. Of particular interest is the online version of the problem (OMRTA), in which tasks in

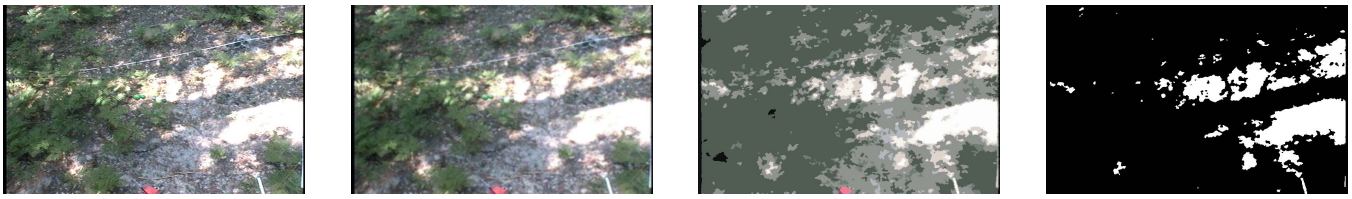

(a) Image captured at 10:00 a.m. (b) Image after noise filtering (c) Segmented gray-scale image (d) Binary image after applying a threshold

Fig. 4: Intermediate results of the Image Processing Algorithm

the environment are geographically and temporally distributed, and robots need to visit task locations to accomplish task completion (sampling). The problem is to assign tasks to robots optimally in an online fashion.

Following the methodology developed in [5], OMRTA consists of assigning available robots to sampling tasks according to an online greedy heuristic that will maximize the utility in a given time epoch. We have implemented two heuristics - *Sampling Area* and *Service Time*. The *Area* heuristic gives priority to sampling tasks of a larger area (i.e. tasks that will glean more information). This heuristic is preferred when the objective is to extract as much information as possible from an unknown environment. The *Time* heuristic, on the other hand, gives priority to tasks that require less service time (sampling time and travel time). This heuristic is useful when the purpose is to sample as many tasks as possible. Hence, the *Time* heuristic is applied when there is a model of a phenomenon distribution (i.e. even one sample of the task is enough to predict its distribution) or when the objective is to cover as many tasks as possible because of spatial variability of the phenomenon.

Note that both the *Time* and *Area* heuristics are online greedy algorithms. It has been shown in [14] that greedy algorithms provide a good approximate solution to online task allocation problems and, in some cases, are within a bounded limit of the optimal solution obtained by offline task allocation algorithms, when the task characteristics are known a priori.

V. Experiments and Analysis

The performance of the multiscale paradigm for sampling light intensity was tested and analyzed through simulations and on a real physical system (please refer to section II).

Images were captured every 15 seconds from a study area located in a field biology station within the mixed conifer forest of the James San Jacinto Mountain Reserve in Southern California [15] between 8:00 a.m. and 8:00 p.m. Note that the physical delay in image acquisition dictates the length of the decision epoch [5] to also equal 15 seconds. A down-looking imager captured snapshots (768x480 pixels) of the understory of a forest canopy covering an area approximately 6 meters in length by 4 meters in width. Images captured between 10:00 a.m. and 11:00 a.m. were analyzed in simulation and using NIMS-3D in a laboratory environment. These images were experimentally verified (by analyzing images during other times of the day and changing the parameters for image processing) to be representative of the spatial and temporal variations occurring in the transect throughout the day. The images captured constitute the information sensed using a high spatial coverage, low-fidelity sensor (imager) and were processed to extract a set of tasks that represent possible regions that could be sampled using the low spatial coverage, high-fidelity PAR sensor carried by the mobile robot.

A. Experiments in Simulation

In simulation, the service time for a particular task was dependent on the sampling time, the sampling density, and the average speed of the mobile robot. We computed the service time in simulation as follows:

$$T_{service} = T_{samp} + T_{travel\_while\_sampling} + T_{inter\_task\_travel}$$
$$= \left\lceil \frac{w}{s} \right\rceil * \left\lceil \frac{h}{s} \right\rceil * t_{samp} + \frac{x_{cm} * \left\lceil \frac{h}{s} \right\rceil + y_{cm}}{v} + \frac{d}{v}$$

where T_{samp} is the sampling time to gather all the samples, $T_{travel\_while\_sampling}$ is the travel time while sampling a given task, $T_{inter\_task\_travel}$ is the time to travel from the previous task to the current task, w and h are the width and height of the bounding rectangle of the current task, x_{cm} and y_{cm} are the width and height in cm of the transect captured in the image, s is the sampling density, t_{samp} is the sampling time to gather one sample, v is the average speed of the mobile robot and d is the distance traveled from the previously serviced task to the current task.

A sampling time of 0.1 seconds to collect one sample worked well for sensing light intensity. The sampling density was varied from $s = 4$ to $s = 20$, where higher values of s imply sparser sampling. For example, when $s = 20$, every 20th pixel is sampled and the rest are linearly interpolated. The average speed of the mobile robot was varied from 40 cm/s to 500 cm/s. We performed experiments for the *Time* and *Area* heuristics. A commitment policy was followed while servicing the tasks. That is, if the robot started servicing a particular task, all the images that arrived while the task was being serviced were ignored. The image that arrived immediately after the task was completely serviced was processed to extract a new set of tasks.

For comparative analysis, performance of each heuristic at each sampling density and average speed was normalized to the absolute performance achievable. To normalize the amount of information sampled in terms of area, the total information available between 10:00 a.m. and 11:00 a.m. was calculated by

(a) Bi-level snapshot of the environment at 10:00 a.m. after applying a threshold to the segmented gray scale image

(b) Reconstructed environment with *Area* as the heuristic and $s = 4$, $v = 40$ cm/s

(c) Reconstructed environment with *Area* as the heuristic and $s = 6$, $v = 40$ cm/s

(d) Reconstructed environment with *Time* as the heuristic and $s = 4$, $v = 40$ cm/s

Fig. 5: Simulation results

taking the difference between consecutive images and counting the number of white pixels in the differenced images. To normalize the amount of information in terms of the number of serviced tasks, the total number of tasks in each processed image was calculated and averaged over each sampling density to get the total number of tasks for a given average speed.

1) Time vs. Area heuristics: Figure 6 shows how the performance of each heuristic (*Area* and *Time*) improves by decreasing the sampling density (increasing the value of s) and increasing the average speed. Decreasing the sampling density results in a greater change in performance as compared to increasing the average speed. A decrease in sampling density results in a decrease in sampling time (T_{samp})as well as a decrease in $T_{travel\_while\_sampling}$. Reduction in $T_{travel\_while\_sampling}$ is due to a decrease in the total linear distance that the node has to travel while performing sampling in the bounding box of the region of interest.

If the performance measure is based on the sampled area, the *Area* heuristic performs better than the *Time* heuristic. This is because for the *Time* heuristic, the majority of time is spent traveling between the tasks. Thus, $T_{inter\_task\_travel}$ is the dominating term, while for the *Area* heuristic it is almost negligible. Since we do not sample while moving in-between tasks, this time is spent without collecting any information from the environment. However, if the performance measure is based on the number of serviced tasks then the *Time* heuristic performs much better. This is because in the *Area* heuristic, the robot is often committed to sampling a task with a large area and may miss several images (and therefore tasks) of the environment.

A snapshot of the sensed regions using area and time heuristics is shown in Figures 5b and 5d. For the area heuristic, it took approximately 7 minutes to sense this region, while for the time heuristic it took approximately 30 seconds to sense all the small regions. Note that if the sensing rate is faster than the rate of change of the phenomena in the environment, then in the limit the two approaches would reconstruct the phenomena with complete fidelity.

Decreasing the sampling density (increasing the value of *s*) results in an improved performance for both heuristics. The improved performance, however, comes at the cost of reconstruction error. From Figures 5b and 5c, one can easily observe that decreasing the sampling density leads to jagged edges for the sampled task (because of linear interpolation) and thus to a larger reconstruction error. The reconstruction error is calculated by counting the number of pixels in the sampled image (after interpolation) that are different from the bi-level form of the input image and is normalized with the total amount of information available in the sampled region. This normalized error ratio is then averaged over all the different speeds of the mobile robot considered, to get an error ratio corresponding to a particular sampling density (*s*). The normalized error ratio for different values of *s* is shown in Figure 7. As expected, reconstruction error increases as sampling density decreases.

We also performed an experiment to compare the performance of a multiscale approach to a traditional full raster scan of the environment. The raster scan samples the complete

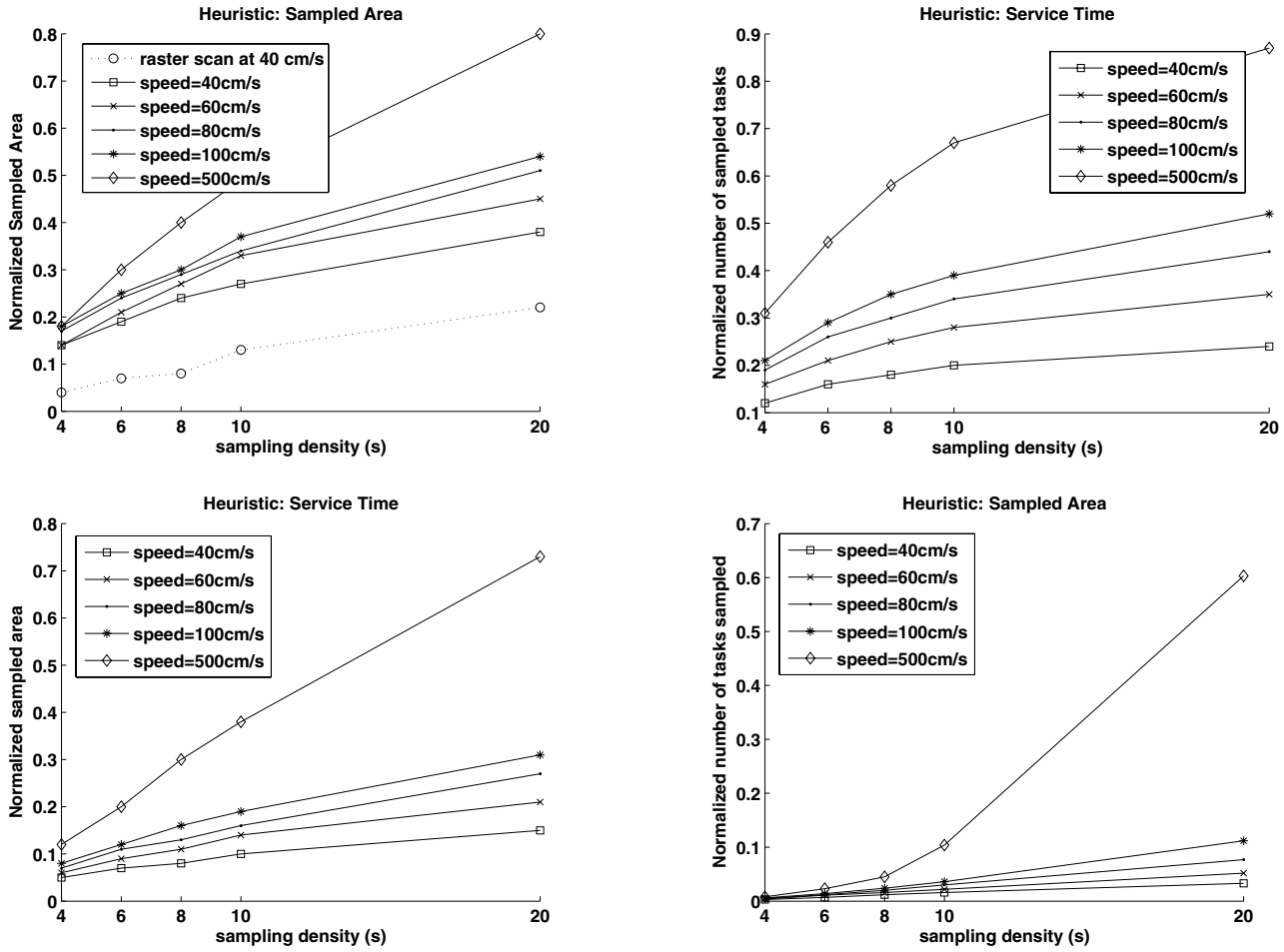

Fig. 6: Simulation results for *Area* and *Time* heuristics. The graphs on the left compare normalized sampled area for different densities and speeds. The graphs on the right compare the normalized number of serviced tasks.

environment with a desired density. We implemented the raster scan with an average speed of 40 cm/s for all sampling densities (the result is shown as dotted line in Figure 6a). Figure 6a illustrates that for corresponding speeds, a multiscale approach performs better than a simple raster scan in terms of the amount of information extracted from the environment. Additionally, the multiscale paradigm yields greater fidelity as well. In the raster scan, the information extracted by sampling the entire transect area initially results in greater error because of the phenomenon dynamics. This is evident, for example, from the number of images processed in the raster scan. They varied from 1 image for $s = 4$ to 9 images for $s = 20$. The total number of images processed (using the same average speed as for the raster scan) using a multiscale approach varied from 13 images for $s = 4$ to 121 images for $s = 20$. Thus, a multiscale approach captures more up-to-date information from the environment resulting in greater fidelity.

2) Multi-Robot Experiments: The performance of a multiscale approach with multiple mobile robots was analyzed in simulation. The sampling density was set to $s = 6$ and the average speed to $v = 60$ cm/s, while the number of robots was varied and the performance was analyzed using

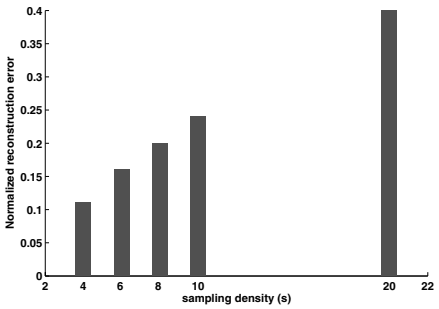

Fig. 7: Reconstruction error for different sampling densities

normalized sampled area. Results are shown in Figure 8. The horizontal line in the graph represents the maximum amount of information that can be extracted at $s = 6$ and $v = 60$ cm/s. This maximum value equals 0.59 while the total maximum amount of information possible is 1. This difference is caused by our commitment policy which results in skipping some images. Initially, an increase in the number of robots results in a proportional increase in the information extracted. However,

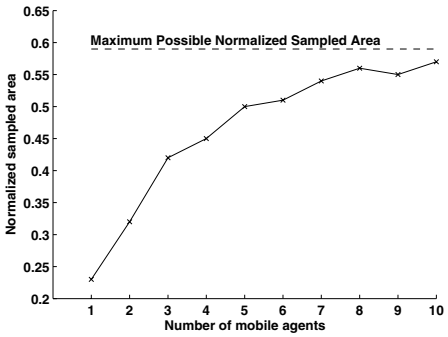

Fig. 8: Performance of multiple mobile sensing robots at s=6 and speed=60 cm/s

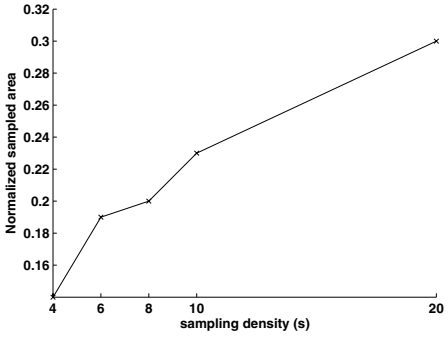

Fig. 9: Performance when interfacing with the real system at different sampling densities

as the number of robots continues to increase, the additional information gathered comes from tasks that have much smaller areas and do not proportionally add new information. As the environment becomes saturated with mobile robots, the system approaches the physical limit in extracting new information.

B. Experiments with the Physical Robotic System

While interfacing with the physical system, we projected the black and white images in a 2-dimensional region that was scanned by the NIMS-3D robot (refer to Section II). The projected image spanned an area of 110 cm in length by 93 cm in height, defining the region in which the mobile node could move. Note that the original image represents an area of $4m$ in height by $6m$ in width in the real environment. Therefore, when implementing our algorithm on a real system, we used an appropriate conversion ratio.

In our experiments, the mobile node achieved a maximum speed of 200 steps/s with a step size of approximately 0.014 cm. The use of a PID controller necessitates a settle or wait-period at the end of each move. The average wait-period was 3 seconds. Position information about the mobile node was generated three times a second while the sampled values from the PAR sensor were collected at 10 Hz. The position information was then interpolated to get a physical location corresponding to each PAR sensor value.

Trends similar to simulation were observed when the two-tier multiscale approach was implemented on a physical system. Results are shown in Figure 9 for a peak speed of 2.4 cm/s. PAR information was also gathered while the node was moving. The intermittent values that were not sampled directly were interpolated.

The NIMS-3D system is developed for general purpose multiscale sampling in many environments. We performed a set of experiments to analyze the reconstruction fidelity achievable with this system at its current state. Figure 10a shows a result of the best possible reconstruction fidelity of the statically projected image shown in Figure 5a. This reconstruction was achieved by sampling points separated in space by 1 cm along both axes. In reality, the robot sampled the PAR continuously while moving in 1 cm increments. The system performed a scan of the environment in around 12 hours. This time performance is prohibitively slow for real world applications.

Alternatively, we performed a much faster scan (around 40 minutes) to sample the complete environment with the sampling density equal to 1 cm along the vertical axis while sampling continuously along the horizontal axis. The horizontal motion from one end to the other was commanded as a single step to the mobile robot. The result of the reconstruction is shown in Figure 10b. Figure 10b shows that considerable reconstruction error is present, which is due to the nonlinear motion and long term positioning drift of the physical system. NIMS-3D is still under development, and experiments with the current system were performed for a proof of concept of interfacing the *multiscale approach* with the real system.

VI. Conclusions and Future Work

We proposed a *multiscale sensing* paradigm for efficiently sampling high frequency spatiotemporally distributed phenomena with high fidelity. We described a two-tier multiscale approach where information from a low-fidelity, high spatial coverage (global) sensor actuates a mobile robotic node, carrying a high-fidelity, low spatial coverage (spot measurement) sensor, to perform guided sampling in the regions of interest (high phenomenon variability).

As a demonstration of the feasibility of this new multiscale method, we investigated a spatiotemporal distribution of light intensity in a forest understory. In this application, we used an imager (a camera) as a first-tier sensor. The imager is a high spatial coverage, low-fidelity sensor that provides global information about the environment. This information is then used to extract the regions of interest. These regions form a set of sampling tasks for second-tier sensors to pursue. This set of tasks is given as an input to the Task Allocation module. The Task Allocation module prioritizes tasks based on the selected utility and assigns the task with the highest utility to the second-tier sensor. The second-tier is represented by mobile robots equipped with high-fidelity low spatial coverage (spot measurement) sensors (PAR sensors). The robots then perform high-fidelity sampling in the regions represented by these tasks.

We implemented a greedy heuristic-based task allocation algorithm in which tasks were prioritized based on a utility

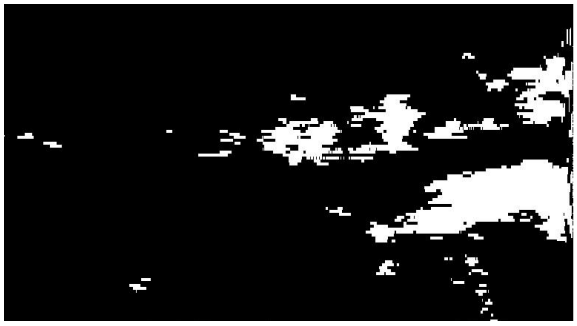

(a) Reconstructed environment from a raster scan of 1 cm along both axises

(b) Reconstructed environment with a continuous scan along the horizontal axis and a 1 cm scan along the vertical axis

Fig. 10: Results using the physical system

(*Area* and *Time*). Simulations showed that if the performance metric is sampled area, the *Area* heuristic performs better than the *Time* heuristic. If the performance metric, however, is the number of serviced tasks then the *Time* heuristic performs better than the *Area* heuristic. Results also showed that decreasing the sampling density (increasing the value of s) resulted in improved performance for both heuristics. The improved performance, however, comes at the cost of increased reconstruction error.

Next, we analyzed how the performance of a multiscale paradigm scales with the number of implicitly coordinated mobile robots operating at the same sampling density and average speed. The experiments show that as the environment becomes saturated with robots, the system approaches the physical limit in extracting new information.

Through simulation we showed that a system using the multiscale paradigm performs better than a traditional sampling technique such as a raster scan. Finally, the multiscale approach was tested on a physical system (NIMS-3D). The performance of the system exhibited behavior similar to that observed in simulation.

In the future, we plan to characterize the task set in order to build a model of future task arrivals and distributions. This would further improve task allocation and, at the limit, yield an optimal solution. We plan to perform phenomena characterization based on the received high-fidelity sensed values. This information can be used to improve first-tier sensor data processing as well as calibration. In theory, if the first-tier sensor is calibrated in accordance with the spatiotemporal nonlinearities in the environment, high fidelity reconstruction of the phenomena may then be extracted entirely from the first-tier sensor. Improvements in NIMS-3D, that will allow larger areas to be sensed, are currently underway.

ACKNOWLEDGMENT

This material is based upon work supported in part by the US National Science Foundation (NSF) under Grants ANI-00331481. Any opinions, findings, and conclusions or recommendations expressed in this material are those of the authors and do not necessarily reflect the views of the NSF.

REFERENCES

[1] D. Estrin, G. Pottie, , and M. Srivastava, "Instrumenting the world with wireless sensor networks," in *IEEE Internatinal Conference on Acoustics Speech and Signal Processing*, Salt Lake City, USA, 2001, pp. VOL 4, pages IV–2033–IV–2036.

[2] M. Rahimi, R. Pon, W. J. Kaiser, G. S. Sukhatmes, D. Estrin, and M. Srivastavan, "Adaptive sampling for environmental robotics," in *IEEE/RSJ International Conference on Intelligent Robots and Systems*, New Orleans, LA, April, 2004, pp. 3537–3544.

[3] A. Singh, R. Nowak, and P. Ramanathan, "Active learning for adaptive mobile sensing networks," in *International Conference on Information Processing in Sensor Networks (to appear)*, Nashville, USA, 2006.

[4] M. A. Batalin, M. Rahimi, Y. Yu, D. Liu, A. Kansal, G. S. Sukhatme, W. J. Kaiser, M. Hansen, G. J. Pottie, M. Srivastava, and D. Estrin, "Call and response: Experiments in sampling the environment," in *ACM Conference on Embedded Networked Sensor Systems*, Maryland, USA, 2004, pp. 25–38.

[5] M. A. Batalin, G. S. Sukhatme, Y. Yu, R. Pon, J. Gordon, M. H. Rahimi, W. J. Kaiser, G. J. Pottie, , and D. E. Estrin, "Task allocation for event-aware spatiotemporal sampling of environmental variables," in *IEEE/RSJ International Conference on Intelligent Robots and Systems*, Edmonton, Canada, 2005, pp. 1846–1853.

[6] C. M. P. Ozanne, D. Anhuf, S. L. Boulter, M. Keller, R. L. Kitching, C. Krner, F. C. Meinzer, A. W. Mitchell, T. Nakashizuka, P. L. S. Dias, N. E. Stork, S. J. Wright, and M. Yoshimura, "Biodiversity meets the atmosphere: A global view of forest canopies," *Science*, vol. 301-5630, pp. 183–186, July 2003.

[7] W. W. Biggs, *Radiation Measurement*. Advanced Agricultural Instrumentation, 1986.

[8] B. P. Gerkey and M. J. Mataric, "A formal analysis and taxonomy of task allocation in multi-robot systems," *International Journal of Robotics Research*, vol. 23-9, pp. 939–954, September 2004.

[9] L. Bianchi, "Notes on dynamic vehicle routing - the state of art. technical report," in *Technical Report,Istituto Dalle Molle di Studi sull'Intelligenza Artificiale*, IDSIA, Switzerland, 2000.

[10] (2005) The NIMS website. [Online]. Available: http://www.cens.ucla.edu/portal/nims.html

[11] P. H. Borgstrom, M. J. Stealey, M. A. Batalin, and W. J. Kaiser, "Nims3d: A novel rapidly deployable robot for 3-dimensional applications," in *IEEE/RSJ International Conference on Intelligent Robots and Systems (Submitted)*, Beijing, China, 2006.

[12] (2006) Open source computer vision library. [Online]. Available: http://www.intel.com/technology/computing/opencv/index.htm

[13] P. J. Burt, T.-H. Hong, and A. Rosenfeld, "Segmentation and estimation of image region properties throuhg cooperative hierarchial computation," in *IEEE Transactions on System, Man, and Cybernetics,*, Dec. 1981, pp. 802–809.

[14] B. Kalyanasundaram and K. Pruhs, "Online weighted matching," *Journal of Algorithms*, vol. 14, pp. 478–488, 1993.

[15] (2005) James san jacinto mountains reserve. [Online]. Available: http://www.jamesreserve.edu